Potential Compounds in Indonesian Herbal Plants using Computational Screening for Inhibitory Activity Against Chikungunya Virus Envelope Protein E2

Inda Setyawati[*], Fatma Ayyalla Fadhilla Ilyas, Mikael Kristiadi, Aprijal Ghiyas Setiawan
Department of Biochemistry, Faculty of Mathematics and Science, IPB University
[*]Email : inda_setyawati@apps.ipb.ac.id

ABSTRACT

Chikungunya disease, marked by fever, headaches, and severe joint pain, is a significant global health issue, especially in tropical and subtropical regions. Despite its prevalence, there is no specific vaccine or drug for Chikungunya, prompting the need for antiviral drug research. This study targets the envelope protein E2 of the Chikungunya virus (CHIKV) using computational methods to identify potential inhibitory compounds from Indonesian herbal compounds. The CHIKV E2 receptor model was constructed using AlphaFold 2, and molecular docking analyses were performed with herbal compounds from the HerbalDB database using AutoDock-GPU. Molecular dynamics (MD) simulations with Gromacs further assessed ligand-protein interactions. Druggable pocket analysis identified 17 potential ligand-binding regions, with Pocket 0 selected for virtual screening. The virtual screening of 3768 herbal compounds identified 23-Hydroxy-mangiferonic acid (a free energy value of -9.0 kcal/mol) as the most promising candidate due to its high binding affinity and stability in molecular dynamics simulations for 250 ns. MD simulations confirmed the stability and specificity of its interactions with key residues in the targeted pocket. The findings suggest that 23-Hydroxy-mangiferonic acid is a promising therapeutic agent against CHIKV, highlighting the effectiveness of computational methods in antiviral drug discovery. This research lays the groundwork for future experimental validation and development of treatments for Chikungunya infections.

Keywords: *Antiviral drug discovery, chikungunya virus, envelope protein E2, Indonesian herbal compounds, molecular docking, molecular dynamics simulations*

1. INTRODUCTION

Chikungunya virus (CHIKV) is an alphavirus in the family *Togaviridae* that is transmitted to humans by *Aedes spp.* mosquitoes. The virus causes infectious disease, characterized by fever, headaches, and joint pains ranging from moderate to severe, poses a significant global health concern[1]. In severe cases, chronic chikungunya can induce prolonged arthralgia, can persist for many months following infection, and has an expected median time to resolution of 6.39 months[2]. Chikungunya spreads rapidly in densely populated tropical and subtropical regions, causing widespread epidemics. Originating in Tanzania in 1952, the virus has since disseminated across Asia and Africa, reaching Indonesia in 1972 and precipitating numerous outbreaks, including a significant event from 2001–2003[3].

In response to this, a vaccine named Ixchiq has been approved for the prevention of CHIKV infection. However, Ixchiq may induce severe, chikungunya-like adverse reactions in some recipients. Additionally, the vaccine's impact on pregnant individuals and the potential risk of transmitting the vaccine virus to newborns could lead to uncertain adverse outcomes[4]. While anti-malarial drugs (chloroquine) have been suggested as potential treatments, their efficacy in halting CHIKV proliferation lacks clinical validation[5]. A promising avenue involves identifying the right receptor as a drug target and conducting virtual screening of candidate compounds, including those sourced from Indonesian herbal plants, known for their rich biodiversity and unique compounds.

The CHIKV spikes are composed of heterodimers of E1 and E2 transmembrane glycoproteins, which are crucial for receptor binding and fusion. E2, in conjunction with E1, facilitates cell entry, with E2 being a primary target for neutralizing antibodies. This process occurs via clathrin-mediated endocytosis, with fusion triggered by the acidic pH environment within the endocytic vesicle[6,7]. These characteristics make E2 a critical target for antiviral therapies against CHIKV involves the inhibition of viral entry mediated by these E1 and E2 proteins.

Structural analyses have identified potential drug targets, and computer-aided drug design has led to the discovery of the potent inhibitors. Computational methods, including structure-based virtual screening and molecular dynamics simulations, have proven instrumental in identifying potential inhibitors, repurposing existing drugs, and discovering novel compounds with antiviral properties[8,9]. These approaches accelerate the discovery of antiviral agents and expand the arsenal of treatments against the chikungunya virus.

This study employs a multifaceted approach, using computational methods to identify potential drug candidates and elucidate their interaction mechanisms with the chikungunya virus (CHIKV). To identify drug targets, the computational construction of the CHIKV E2 receptor model using AlphaFold2 was conducted, followed by molecular docking analyses utilizing a library of herbal compounds sourced from the HerbalDB database. Molecular docking investigations were carried out using Autodock-GPU, and further assessment of ligand-protein interactions was performed through MD simulations of CHIKV E2 using Gromacs software.

2. MATERIALS AND METHODS

This research was conducted at the Department of Biochemistry, IPB University (-6.557210422237054, 106.72532696759797).

Structure modeling

The receptor model of CHIKV E2 was constructed using AlphaFold 2.0[10] with ColabFold as the platform[11], an open-source implementation that simplifies the use of AlphaFold for protein structure prediction. The receptor model was then prepared for further analysis using the AutoDock Tools program[12].

Drugability analysis

Drugability analysis was performed to predict the binding regions of candidate herbal drug compounds by evaluating protein pocket characteristics using the DoGSiteScore server[13]. The best pockets for ligand binding were selected based on a pocket score greater than 0.5.

Ligand preparation

To identify potential drug candidates, molecular docking analysis was conducted using a library of herbal compounds from the HerbalDB database. Ligand data were retrieved using a Python script with the Selenium library to scrape information such as compound names, Knapsack IDs, and plant species names. Knapsack IDs were used to extract additional data from the KNApSAcK Family database. The Gypsum-DL program was then employed to generate 3D structures of the compounds from their SMILES representations, which were stored in SDF and PDB formats for virtual screening.

Molecular docking analysis

Molecular docking investigations were carried out using Autodock-GPU on Google Colab Pro platforms. The ligand dataset was docked into the selected pocket of the capsid proteins using AutoDock4, enhanced by OpenCL and Cuda for improved performance. A grid parameter file (GPF) was generated using the AutoDock Tools program[14]. The grid box size was validated with a spacing value of 0.375 Å, and the optimal size between 40-85 Å was determined. The grid box tool was used to validate the size, and the center of the grid box was determined in the x, y, and z columns. Parameters used in Autodock 4 included the size and position of the box, the number of grid points, grid spacing, number of genetic algorithm (GA) runs, population size, maximum energy evaluations, and maximum generations.

Molecular dynamics analysis

Molecular dynamics (MD) simulation was conducted using an HPC (NVIDIA DGX A100) cluster at the Advanced Research Laboratory, IPB University. The MD of the CHIKV E2 in aqueous salt solutions were performed with the selected ligand. The predicted AlphaFold2 structure served as the initial model for the E2 protein. All-atom MD simulations were conducted using the Gromacs package (version 2020)[15,16] with the CHARMM36 force field[17]. The protein model was placed in a cubic box, solvated and neutralized. After solvation, the system underwent energy minimization using the steepest descent algorithm until the maximum force was reduced to 1000 kJ mol^{-1} nm^{-1}. The systems were optimized and equilibrated for at least 1 ns in the NVT ensemble. Subsequently, the system was simulated with restraints for 20 ns twice in the NPT ensemble using the Nose-Hoover thermostat and the Parrinello-Rahman barostat at a reference temperature and pressure of 303.15 K and 1 bar, respectively. The production run was performed for 250 ns in the NPT ensemble (constant pressure, constant temperature) without backbone restraints. Non-bonded interactions were treated using the Verlet cut-off scheme, with the particle mesh Ewald (PME) method for long-range electrostatic interactions, and a 12 Å cut-off for short-range electrostatic and van der Waals interactions. Periodic boundary conditions were applied to all simulations, and bonds involving hydrogen atoms were constrained using

the linear constraint-solving (LINCS) algorithm.

MD analysis

The temporal evolution of the interaction distances between CHIKV E2 and the ligand was analyzed based on the center of geometry of the His29 and Arg13 residues relative to the ligand's center of geometry. Visual inspection of the trajectories was performed using VMD and PyMOL (DeLano Scientific, Palo Alto, CA, USA).
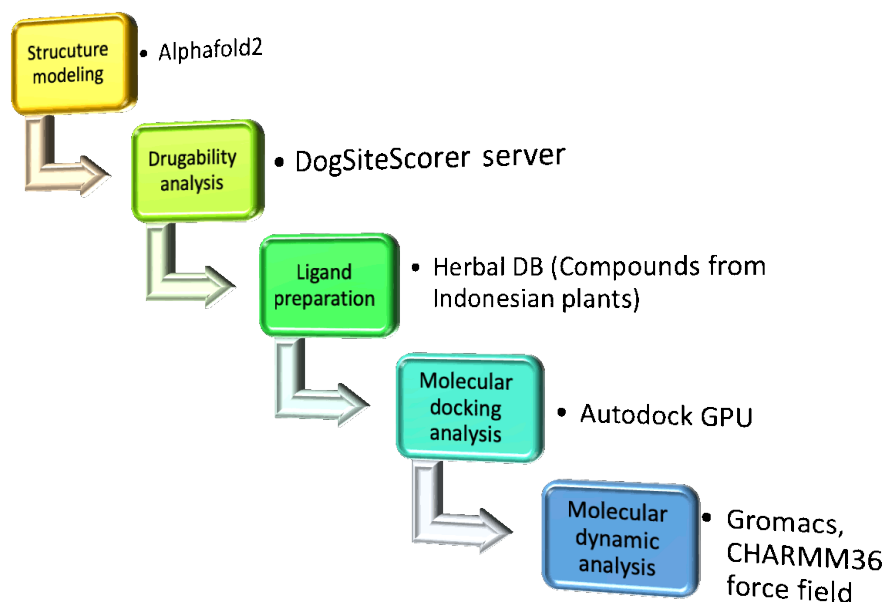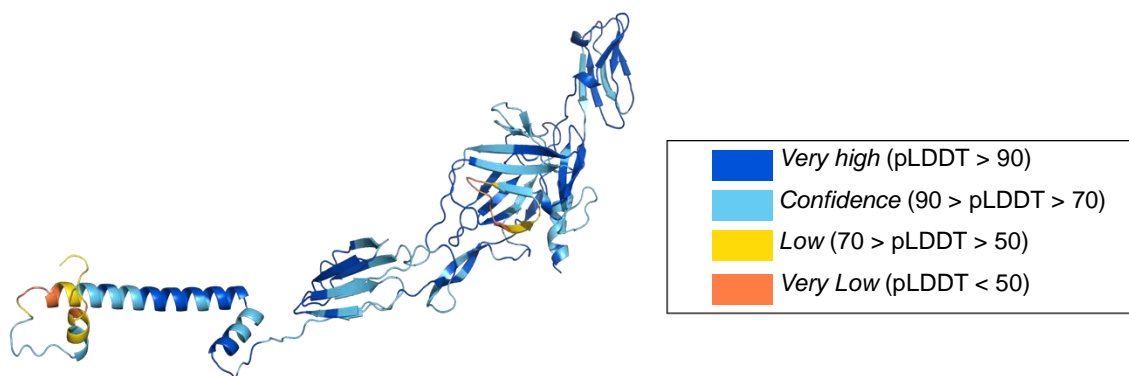

Figure 1. Research flow diagram

3. RESULTS AND DISCUSSION
The Characteristics of the Receptor Model

The structural modeling of the Chikungunya virus envelope protein E2 using AlphaFold2 demonstrated a reasonably high confidence level, as indicated by the abundance of blue colors with pLDDT values ranging between 70 to 90 (Figure 1).

Figure 2. The model structure of E2 predicted by Alphafold2.

A druggable pocket analysis identified potential ligand-binding regions on the surface of the E2 protein, which are critical for effective drug targeting. The analysis utilized the protein.plus server in the DoGSiteScorer tools, resulting in the identification of 17 pockets. Table 1 summarizes the analysis results for several pockets on the E2 receptor, specifically Pocket 0 (P0), Pocket 1 (P1), Pocket 2, Pocket 3, and Pocket 6, all of which obtained good drug scores greater than 0.5. In this study, Pocket 0 was chosen as the binding region for virtual screening (Figure 2A). This pocket not only had a good drug score but also a substantial surface area of 854.3 Å³. Pocket 0 contains residues suitable for antigen attachment, including those in the FG Loop, Beta-Hairpin, BC Loop, and EBA Strand (Figure 2B), marked by the presence of residues Pro176, Leu16, His29, Asn72, Asp71, Lys120, and Arg178.
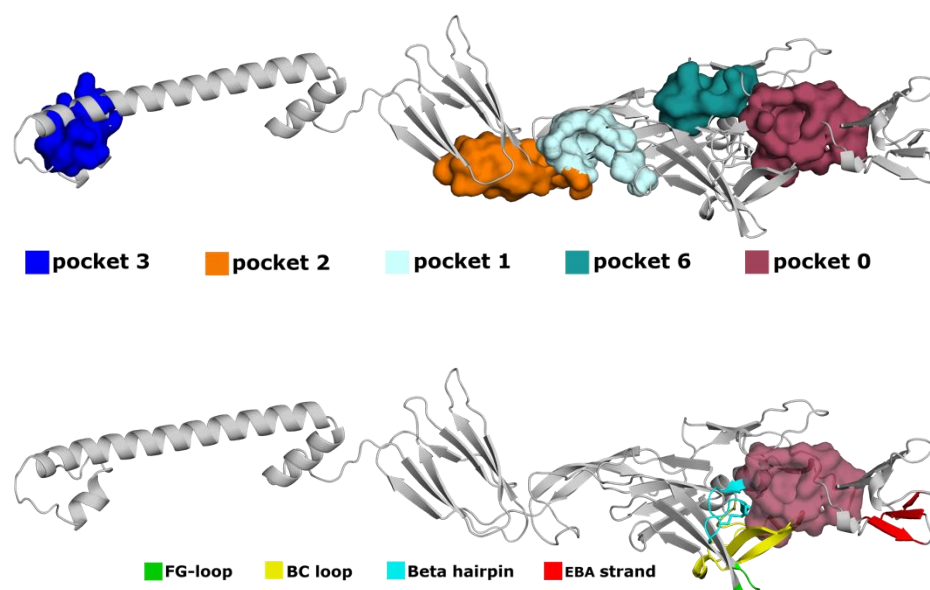
Figure 3. The drugable pocket on envelope E2 highlights the potential pockets for therapeutic compounds (top) and the region for antigen attachment surrounding pocket 0, indicating where antigens can bind to the envelope protein (below)

Tabel 1 pocket analysis parameters on the E2 receptor

Pocket	Volume ($Å^2$)	Wide area ($Å^3$)	*Drug Score*	*Simple Score*
0	854.3	1066.34	0.77	0.57
1	481.34	615.49	0.73	0.27
2	383.43	383.43	0.81	0.23
3	335.61	335.61	0.64	0.25
4	273.07	273.07	0.47	0.19
5	261.75	261.75	0.45	0.16
6	223.55	273.07	0.51	0.0
7	179.41	179.41	0.33	0.19
8	156.2	156.2	0.35	0.0
9	146.3	146.3	0.34	0.01
10	144.32	234.92	0.28	0.02
11	132.43	329.65	0.0	0.0

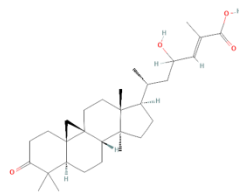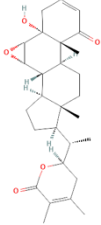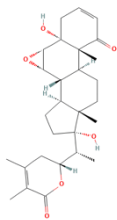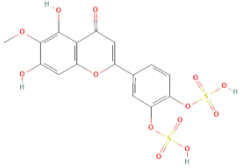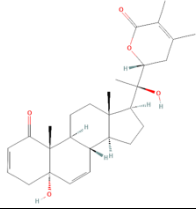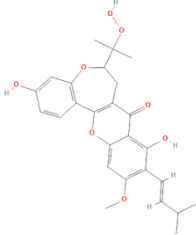| Pocket	Volume (Å²)	Wide area (Å³)	*Drug Score*	*Simple Score*
12	128.47	314.43	0.0	0.0
13	125.36	193.04	0.0	0.0
14	118.0	214.7	0.0	0.0
15	116.87	116.87	0.0	0.0
16	116.59	116.59	0.0	0.0
17	108.66	108.66	0.0	0.0

Potential inhibitory compounds
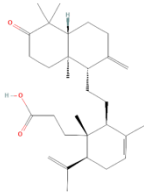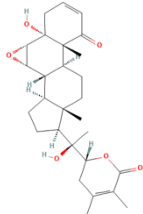
Virtual screening was the initial stage in filtering active compounds (ligands) from a total of 3768 compounds retrieved from the HerbalDB and KNApSAcK databases. The selected compounds had molecular weights of less than 500 Da and were predictively capable of interacting with catalytic residues. Virtual screening using Autodock 4 employed a grid box size of 85 x 85 x 85, targeting potential binding sites, specifically pocket 0 within the antigenic region (Figure 2B). The chosen parameters for the center coordinates were x = 15.317, y = 11.293, and z = -11.329. Table 5 presents the results of virtual screening by AutoDock 4, listing the top 10 compounds based on the lowest free energy (ΔG) that exhibit promising potential for further investigation in drug development studies. The ranking results using the Autodock4 algorithm revealed that 23-Hydroxy-mangiferonic acid (from Garcinia cornea and Mangifera indica) exhibited the highest binding affinity with a free energy value of -9.0 kcal/mol. Additionally, other selected compounds included Lansionic acid (from Lansium domesticum) and Withanolide A (from Withania somnifera) with free energy values of -8.9 kcal/mol.

23-Hydroxy-mangiferonic acid is a cycloartane triterpenoid compound with anti-melanin deposition activity by downregulating tyrosinase gene expression. This compound has been isolated and structurally characterized from the bark of G. cornea[18] and *M. indica* (Anjaneyulu et al., 1999). Although the potential of 23-Hydroxy-mangiferonic acid as a drug candidate has not been extensively investigated, it theoretically fulfills all of Lipinski's rules (Table 2). The comprehensive analysis of these top compounds, along with their bioavailability predictions, highlights their potential as viable drug candidates for further experimental validation and development.

Tabel 1. The 10 top ligands identified through virtual screening

No	Compounds (Plant species)	Binding energy (*ΔG*)	Molecular weight	Structure
1	*23-Hydroxy-mangiferonic acid (Garcinia cornea, Mangifera indica)*	-9.0	470.3396	

No	Compounds (Plant species)	Binding energy (*ΔG*)	Molecular weight	Structure
2	*Lansionic acid* *(Lansium domesticum)*	-8.91	456.3603	
3	*Withanolide A* *(Withania somnifera)*	-8.91	470.2668	
4	*Lycium substance B* *(Withania somnifera)*	-8.85	454.2719	
5	*Withanone* *(Withania somnifera)*	-8.82	470.2668	
6	*6-Methoxyluteolin 3',4'-disulfate* *(Lippia nodiflora)*	-8.82	475.9719	
7	*Withacoagin* *(Withania somnifera)*	-8.75	454.2719	
8	*Artoindonesianin B* *(Artocarpus champeden)*	-8.71	468.1784	
No	Compounds	Binding	Molecular	Structure
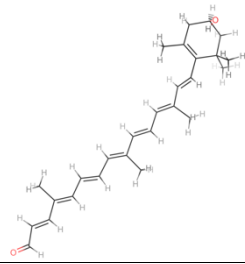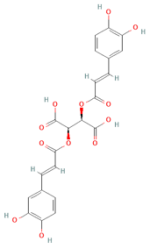
	(Plant species)	energy (*ΔG*)	weight	
9	*Apo-10'-zeaxanthinal (Capsicum annuum)*	-8.65	392.2715	
10	*Chicoric acid (Cichorium endivia, Cichorium intybus, Lactuca sativa)*	-8.65	474.0798	

Table 2. Bioavailability prediction of the 10 top compounds based on the Lipinski rule

Ligand	Molecular weight (Da)	The number of hydrogen bond donor	The number of hydrogen bond acceptor	Log P	Molar refractivity
23-Hydroxy-mangiferonic acid (Garcinia cornea, Mangifera indica)	470	2	4	6.4126	133.07
Lansionic acid (Lansium domesticum)	456	2	3	7.5658	136.86
Withanolide A (Withania somnifera)	470	2	6	3.4953	124.51
Lycium substance B (Withania somnifera)	454	1	5	4.3804	123.05
Withanone (Withania somnifera)	470	2	6	3.4953	124.51
6-Methoxyluteolin 3',4'-disulfate (Lippia nodiflora)	476	4	13	3.2474	100.14
Withacoagin (Withania somnifera)	454	2	5	4.2841	124.99
Artoindonesianin B (Artocarpus champeden)	468	3	8	5.1813	125.34
Apo-10'-zeaxanthinal (Capsicum annuum)	392	1	2	6.7464	125.61
Chicoric acid (Cichorium endivia, Cichorium intybus, Lactuca sativa)	474	6	12	1.2284	112.64

▆ = deviates from Lipinski's rule

Molecular docking pose of 23-hydroxy-mangiferonic acid in the targeted pocket

The dynamic interactions of 23-Hydroxy-mangiferonic acid with residues in the E2 protein complex were thoroughly analyzed using various distance and fluctuation measurements over a 200 ns simulation. These measurements provide insights into the stability and behavior of the ligand-protein interactions under physiological conditions.

The distance between atom H111 in the ligand and NE2 in His-29 initially shows a stable interaction, maintaining around 10 Å. This distance gradually increases to approximately 20 Å with noticeable fluctuations. Between 50 and 200 ns, the distance fluctuates between 15 and 30 Å, indicating a relatively stable yet dynamic interaction. A significant spike occurs around 200 ns, where the distance rapidly increases to 50 Å, suggesting a temporary dissociation or large conformational change. Post this event, the distance returns to ar 331 Å, signifying a possible re-estab of the interaction or a transition to a new stable state. This behavior indicates the resilience of the ligand in maintaining interactions with His-29, which is critical for its inhibitory potential.

Similarly, the distance between atom O3 in the ligand and HH21 in Arg-13 remains below 10 Å for most of the simulation, with minor fluctuations indicating a stable interaction. A substantial spike occurs around 200 ns, reaching 50 Å, mirroring the behavior seen with the His-29 interaction. This parallel behavior suggests that both His-29 and Arg-13 interactions are affected by a major conformational change around the 200 ns mark, significantly impacting their interactions with the ligand. This finding aligns with previous studies on ligand-protein dynamics, where significant conformational changes are observed in response to environmental shifts.

The RMSF analysis reveals regions of high flexibility in the protein, particularly around residues 200 and 400. These flexible regions could correlate with the fluctuations observed in the distance measurements, suggesting areas of the protein undergoing significant motion during the simulation. High RMSF values at specific residues indicate adaptability, which might facilitate binding by allowing the protein to conform to the ligand's shape. Previous research has shown that such flexibility is crucial for effective ligand binding, as it allows the protein to accommodate different conformations of the ligand.

The RMSD data provides an overview of the structural deviations over time. Initially, the RMSD increases from low values to around 20 Å, reflecting an initial structural adjustment. The RMSD stabilizes with fluctuations, then shows a notable drop around 200 ns before increasing again. This pattern suggests an initial conformational change leading to a new stable structure, followed by a major event around 200 ns that corresponds with the dissociation events seen in the distance measurements. The RMSD drop suggests a transient return to a less deviated state, potentially aligning with the ligand re-binding or structural realignment. Similar patterns have been observed in other protein-ligand systems, where significant conformational changes are followed by re-stabilization.

The ligand forms several strong interactions with the protein, including conventional hydrogen bonds with Leu16 and Arg13 residues, and various hydrophobic interactions such as pi-sigma interactions with His29, alkyl interactions with Leu16, Pro243, and Val242, and pi-alkyl interactions with Tyr15, His29, and His73. These interactions are crucial for the stability and specificity of the binding, providing multiple points of contact that enhance binding affinity. The importance of these interactions has been highlighted in several studies, which demonstrate that

multiple contact points are essential for the high binding affinity and stability of protein-ligand complexes[19].

Given the stability of interactions (with fluctuations largely within an acceptable range), the ability of the ligand to re-establish interactions after a significant conformational event, the adaptive flexibility of the binding pocket, and the multiple strong binding interactions (hydrogen bonds and hydrophobic interactions), it can be concluded that the binding of 23-Hydroxy-mangiferonic acid to the targeted pocket is indeed favorable. The dynamic nature of the protein-ligand interactions, as evidenced by the data, supports the notion that 23-Hydroxy-mangiferonic acid can effectively and stably bind to the targeted pocket in the E2 protein complex. This conclusion is consistent with findings from other studies on ligand dynamics and binding stability[20].
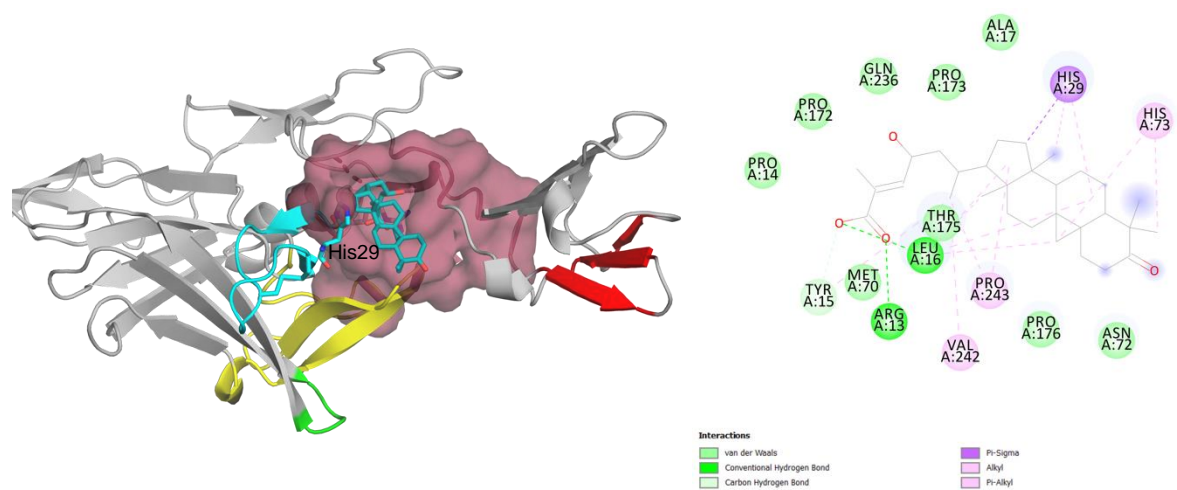
Figure 4. The docking pose (left) and 2D interaction diagram (right) of 23-hydroxy-mangiferonic acid (*G. cornea* and *M. indica*) on the targeted pocket of CHIKV E2.
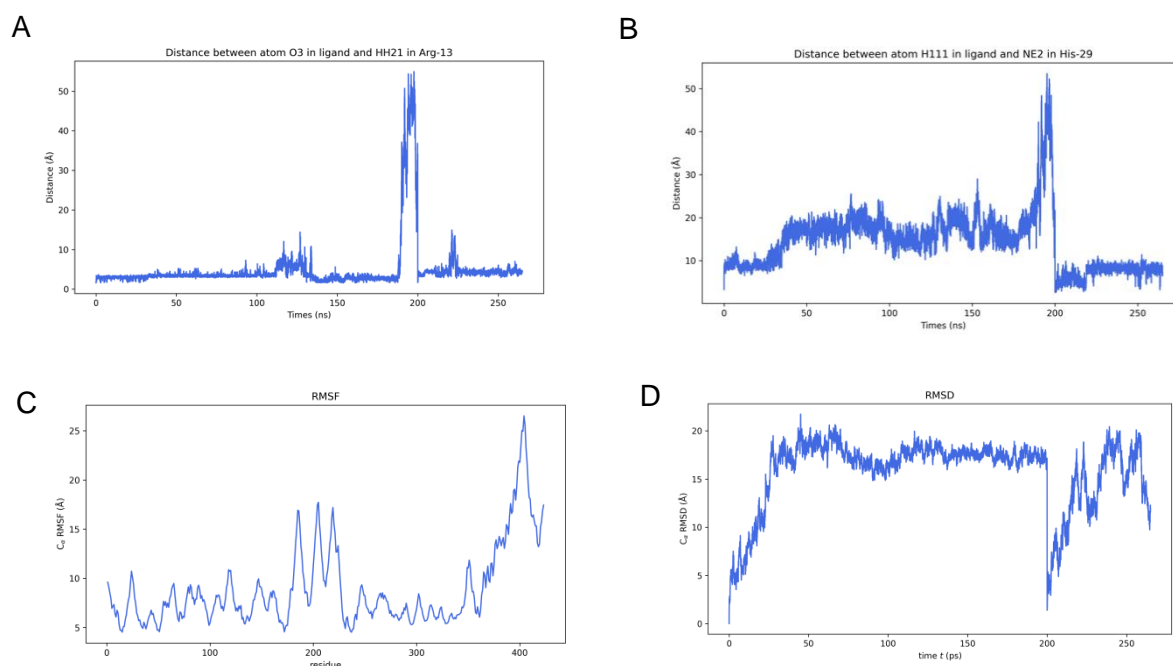
Figure 5. The MD analysis (250 ns) of 23-hydroxy-mangiferonic acid (*Garcinia cornea* and *Mangifera indica*) on the targeted pocket of CHIKV E2: A. Distance between atom O3 in the ligand and HH21 in Arg13; B. Distance between atom H111 in the ligand and NE2 in His-29; C. Root Mean Square Fluctuation (RMSF); D. Root Mean Square Deviation (RMSD).

4. CONCLUSION

This study employed a comprehensive computational approach to identify potential inhibitory compounds against the Chikungunya virus (CHIKV) by targeting the envelope protein E2, highlighting the potential of 23-Hydroxy-mangiferonic acid as a promising therapeutic candidate. Using AlphaFold2 for structural modeling, druggable pockets on the E2 protein were identified, with Pocket 0 being selected for virtual screening due to its high drug score and substantial surface area. Virtual screening of 3768 herbal compounds from the HerbalDB and KNApSAcK databases highlighted 23-Hydroxy-mangiferonic acid as the most promising candidate, demonstrating the highest binding affinity with a free energy value of -9.0 kcal/mol.

Molecular dynamics simulations further confirmed the stability and specificity of the interactions between 23-Hydroxy-mangiferonic acid and key residues within Pocket 0. The dynamic nature of these interactions, along with the strong binding affinities, suggests that 23-Hydroxy-mangiferonic acid has significant potential as a therapeutic agent against CHIKV. The findings underscore the importance of computational methods in accelerating the discovery of antiviral agents, providing a solid foundation for future experimental validation and development of effective treatments for Chikungunya virus infections.

These results demonstrate that targeting the E2 protein of CHIKV with specific inhibitors can be a viable strategy

for antiviral therapy development. The use of computational tools like molecular docking and dynamics simulations proves to be an efficient method for screening and identifying potential antiviral compounds, especially from natural sources. The promising binding affinity and interaction stability of 23-Hydroxy-mangiferonic acid encourage further experimental studies to validate its efficacy and explore its potential as a lead compound in drug development against CHIKV.

ACKNOWLEDGEMENT

REFERENCES

Abraham, M. J.; Murtola, T.; Schulz, R.; Páll, S.; Smith, J. C.; Hess, B.; Lindahl, E. GROMACS: High Performance Molecular Simulations through Multi-Level Parallelism from Laptops to Supercomputers. *SoftwareX* **2015**, *1–2*, 19–25. https://doi.org/10.1016/j.softx.2015.06.001.

Afreen, N.; Deeba, F.; Naqvi, I.; Shareef, M.; Ahmed, A.; Broor, S.; Parveen, S. Molecular Investigation of 2013 Dengue Fever Outbreak from Delhi, India. *PLoS Curr* **2014**. https://doi.org/10.1371/currents.outbreaks.0411252a8b82aa933f6540abb54a855f.

Amaral, J. K.; Bilsborrow, J. B.; Schoen, R. T. Brief Report: The Disability of Chronic Chikungunya Arthritis. *Clin Rheumatol* **2019**, *38* (7), 2011–2014. https://doi.org/10.1007/s10067-019-04529-x.

Battini, L.; Fidalgo, D. M.; Álvarez, D. E.; Bollini, M. Discovery of a Potent and Selective Chikungunya Virus Envelope Protein Inhibitor through Computer-Aided Drug Design. *ACS Infect Dis* **2021**, *7* (6), 1503–1518. https://doi.org/10.1021/acsinfecdis.0c00915.

Forli, S.; Huey, R.; Pique, M. E.; Sanner, M. F.; Goodsell, D. S.; Olson, A. J. Computational Protein–Ligand Docking and Virtual Drug Screening with the AutoDock Suite. *Nat Protoc* **2016**, *11* (5), 9~~05~~ ~~2~~. https://doi.org/10.1038/nprot 51.

Holmes, A. C.; Basore, K.; Fremont, D. H.; Diamond, M. S. A Molecular Understanding of Alphavirus Entry. *PLoS Pathog* **2020**, *16* (10), e1008876. https://doi.org/10.1371/journal.ppat.1008876.

Huang, J.; MacKerell, A. D. CHARMM36 All-Atom Additive Protein Force Field: Validation Based on Comparison to NMR Data. *J Comput Chem* **2013**, *34* (25), 2135–2145. https://doi.org/10.1002/jcc.23354.

Huang, Y.; Yang, C.; Xu, X.; Xu, W.; Liu, S. Structural and Functional Properties of SARS-CoV-2 Spike Protein: Potential Antivirus Drug Development for COVID-19. *Acta Pharmacol Sin* **2020**, *41* (9), 1141–1149.

334

https://doi.org/10.1038/s41401-020-0485-4.

Jumper, J.; Evans, R.; Pritzel, A.; Green, T.; Figurnov, M.; Ronneberger, O.; Tunyasuvunakool, K.; Bates, R.; Žídek, A.; Potapenko, A.; Bridgland, A.; Meyer, C.; Kohl, S. A. A.; Ballard, A. J.; Cowie, A.; Romera-Paredes, B.; Nikolov, S.; Jain, R.; Adler, J.; Back, T.; Petersen, S.; Reiman, D.; Clancy, E.; Zielinski, M.; Steinegger, M.; Pacholska, M.; Berghammer, T.; Bodenstein, S.; Silver, D.; Vinyals, O.; Senior, A. W.; Kavukcuoglu, K.; Kohli, P.; Hassabis, D. Highly Accurate Protein Structure Prediction with AlphaFold. *Nature* **2021**, *596* (7873), 583–589. https://doi.org/10.1038/s41586-021-03819-2.

Liang, L.; Ahamed, A.; Ge, L.; Fu, X.; Lisak, G. Advances in Antiviral Material Development. *Chempluschem* **2020**, *85* (9), 2105–2128. https://doi.org/10.1002/cplu.202000460.

Majewski, M.; Barril, X. Structural Stability Predicts the Binding Mode of Protein–Ligand Complexes. *Journal of Chemical Information and Modeling*. 2020. https://doi.org/10.1021/acs.jcim.9b01062.

Mirdita, M.; Schütze, K.; Moriwaki, Y.; Heo, L.; Ovchinnikov, S.; Steinegger, M. ColabFold: Making Protein Folding Accessible to All. *Nat Methods* **2022**, *19* (6), 679–682. https://doi.org/10.1038/s41592-022-01488-1.

Morris, G. M.; Huey, R.; Lindstrom, W.; Sanner, M. F.; Belew, R. K.; Goodsell, D. S.; Olson, A. J. Software News and Updates AutoDock4 and AutoDockTools4 : Automated Docking with Selective Receptor Flexibility. **2009**. https://doi.org/10.1002/jcc.

Nugroho, A. E.; Matsumoto, M.; Sotozono, Y.; Kaneda, T.; Hadi, A. H. A.; Morita, H. Cycloartane Triterpenoids With Anti-Melanin Deposition Activity. *Natural Product Communications*. 2018. https://doi.org/10.1177/1934578x1801300706.

O'Driscoll, M.; Salje, H.; Chang, A. Y.; Watson, H. Arthralgia Resolution Rate Following Chikungunya Virus Infection. *International Journal of Infectious Diseases* **2021**, *1* https://doi.org/10.1016/j.ijid. .066.

Pronk, S.; Páll, S.; Schulz, R.; Larsson, P.; Bjelkmar, P.; Apostolov, R.; Shirts, M. R.; Smith, J. C.; Kasson, P. M.; van der Spoel, D.; Hess, B.; Lindahl, E. GROMACS 4.5: A High-Throughput and Highly Parallel Open Source Molecular Simulation Toolkit. *Bioinformatics* **2013**, *29* (7), 845–854. https://doi.org/10.1093/bioinformatics/btt055.

Smith, G. R.; Sternberg, M. J. E. Prediction of Protein–Protein Interactions by Docking Methods. *Current Opinion in Structural Biology*. 2002. https://doi.org/10.1016/s0959-440x(02)00285-3.

Van Duijl-Richter, M.; Hoornweg, T.; Rodenhuis-Zybert, I.; Smit, J. Early Events in Chikungunya Virus

335

Infection—From Virus CellBinding to Membrane Fusion. *Viruses* **2015**, *7* (7), 3647–3674. https://doi.org/10.3390/v7072792.

Volkamer, A.; Kühn, D.; Grombacher, T.; Rippmann, F.; Rarey, M. Combining Global and Local Measures for Structure-Based Druggability Predictions. *Journal of Chemical Information and Modeling*. 2012. https://doi.org/10.1021/ci200454v

Wahid, B.; Ali, A.; Rafique, S.; Idrees, M. Global Expansion of Chikungunya Virus: Mapping the 64-Year History. *International Journal of Infectious Diseases* **2017**, *58*, 69–76. https://doi.org/10.1016/j.ijid.2017.03.006.